

## Irradiation of Imine–Group VI Carbene Complexes in the Presence of Alkynes: A Theoretical and Experimental Study

Pedro J. Campos, Diego Sampedro, and Miguel A. Rodríguez\*

Departamento de Química, Universidad de La Rioja, Grupo de Síntesis Química de La Rioja, Unidad Asociada al C.S.I.C.; Madre de Dios, 51, E-26006 Logroño, Spain

miguelangel.rodriguez@dq.unirioja.es

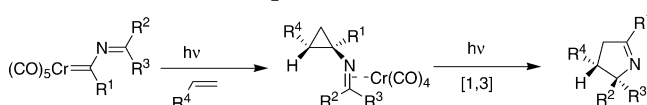
Received March 8, 2003

The photoreaction between imine-substituted Fischer carbene complexes and alkynes is studied at both experimental and theoretical levels. 2*H*-Pyrrole derivatives are easily obtained as main products in moderate to good yields, with complete control of the regiochemistry. High-level theoretical calculations are carried out in order to explore and fully understand the reaction pathway. On the basis of the theoretical results, a mechanism that accounts for the experimental findings is proposed.

### Introduction

The use in synthesis of complexes of the type  $(\text{CO})_5\text{M}=\text{C}(\text{X})\text{R}$  (M = group VI metal; X =  $\pi$ -donor substituent, usually with an O or N atom bonded to the metal; R = alkyl, alkenyl, alkynyl or aryl group), although relatively recent, has shown impressive potential.<sup>1</sup> These compounds, called Fischer carbene complexes after their discoverer,<sup>2</sup> have been shown to be extremely versatile organometallic reagents with an extensive chemistry including cycloadditions of almost any kind.<sup>3</sup> More recently, the photochemistry of group VI carbene complexes has emerged as a new and very valuable route toward different kinds of compounds such as cyclobutanones and  $\beta$ -lactams.<sup>4</sup> As part of our efforts to further develop the synthetic utility of the photoreactivity of carbene complexes, we reported in preceding papers the cycloaddition of imine-substituted carbene complexes with alkenes and

### SCHEME 1. Photoreactivity of Chromium Imine–Carbene Complexes with Alkynes



alkynes<sup>5</sup> and heteroatom-containing double bonds.<sup>6</sup> Thorough research<sup>7</sup> of the reaction with olefins, including the synthetic scope and the first photochemical study for this kind of compounds, showed that this reaction actually consists of two different, consecutive photochemical reactions, the first one leading to a cyclopropane, which subsequently rearranges<sup>7b</sup> to finally give the observed 1-pyrrole (Scheme 1).<sup>7</sup> While it has been possible to clarify the mechanism for the reaction of imine–carbene complexes with alkenes, the corresponding cycloaddition with alkynes still has some controversial points. In contrast with the well-studied benzannulation procedures of Fischer carbene complexes via both the experimental<sup>8</sup> and theoretical<sup>9</sup> approaches, there is no mechanistic study of the cyclopentannulation of imine–group VI carbene complexes with alkynes, thermal or photochemical. This reaction seems to be related to other cyclization processes produced by Fischer carbene complexes, such as the Dötz benzannulation. However, there are some characteristics that make this reaction different. In particular, the products obtained *never* include a CO from the metal part. Therefore, the final products have five-membered cycles, in contrast to the six-membered cycles of the Dötz reaction, which are usually the main product.

(1) For reviews, see: (a) Barluenga, J.; Suárez-Sobrinó, A. L.; Tomás, M.; García-Granda, S.; Santiago-García, R. *J. Am. Chem. Soc.* **2001**, *123*, 10494. (b) Davies, M. W.; Johnson, C. N.; Harrity, J. P. A. *J. Org. Chem.* **2001**, *66*, 3525. (c) Sierra, M. A. *Chem. Rev.* **2000**, *100*, 3591. (d) Dörwald, F. Z. *Carbenes in Organic Chemistry*; Wiley-VCH: Weinheim, 1999. (e) Dötz, K. H.; Tomuschat, P. *Chem. Soc. Rev.* **1999**, *28*, 187. (f) Barluenga, J. *Pure Appl. Chem.* **1999**, *71*, 1385. (g) Aumann, R.; Nienaber, H. *Adv. Organomet. Chem.* **1997**, *41*, 163. (h) Barluenga, J. *Pure Appl. Chem.* **1996**, *68*, 543. (i) de Meijere, A. *Pure Appl. Chem.* **1996**, *68*, 61. (j) Harvey, D. F.; Sigano, D. M. *Chem. Rev.* **1996**, *96*, 271. (k) Hegedus, L. S. In *Comprehensive Organometallic Chemistry II*; Abel, E. W., Stone, F. G. A., Wilkinson, G., Eds.; Pergamon Press: Oxford, 1995; Vol. 12, p 549. (l) Wulff, W. D. In *Comprehensive Organometallic Chemistry II*; Abel, E. W., Stone, F. G. A., Wilkinson, G., Eds.; Pergamon Press: Oxford, 1995; Vol. 12, p 469. (m) Wulff, W. D. In *Comprehensive Organic Synthesis*; Trost, B. M., Fleming, I., Eds.; Pergamon Press: Oxford, 1991; Vol. 5, p 1065. (n) Dötz, K. H. *Angew. Chem.* **1984**, *96*, 573; *Angew. Chem., Int. Ed. Engl.* **1984**, *23*, 587. (o) Dötz, K. H.; Fischer, H.; Hofmann, P.; Kreissl, F. R.; Schubert, U.; Weiss, K. *Transition Metal Carbene Complexes*; VCH: Weinheim, 1983.

(2) Fischer, E. O.; Maasböl, A. *Angew. Chem.* **1964**, *76*, 645; *Angew. Chem., Int. Ed. Engl.* **1964**, *3*, 580.

(3) (a) Barluenga, J.; Martínez, S.; Suárez-Sobrinó, A. L.; Tomás, M. *J. Am. Chem. Soc.* **2001**, *123*, 11113. (b) Barluenga, J.; Tomás, M.; Rubio, E.; López-Peigrin, J. A.; García-Granda, S.; Priede, M. P. *J. Am. Chem. Soc.* **1999**, *121*, 3065. (c) Frühauf, H. W. *Chem. Rev.* **1997**, *97*, 523. (d) Schmalz, H.-G. *Angew. Chem.* **1994**, *106*, 311; *Angew. Chem., Int. Ed. Engl.* **1994**, *33*, 303.

(4) For a review, see: Hegedus, L. S. *Tetrahedron* **1997**, *53*, 4105.

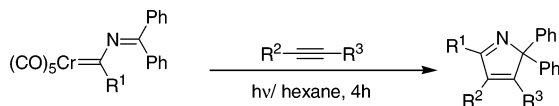
(5) Campos, P. J.; Sampedro, D.; Rodríguez, M. A. *Organometallics* **2000**, *19*, 3082.

(6) Campos, P. J.; Sampedro, D.; Rodríguez, M. A. *Tetrahedron Lett.* **2002**, *43*, 73.

(7) (a) Campos, P. J.; Sampedro, D.; Rodríguez, M. A. *Organometallics* **2002**, *21*, 4076. (b) Campos, P. J.; Soldevilla, A.; Sampedro, D.; Rodríguez, M. A. *Org. Lett.* **2001**, *3*, 4087.

(8) For a review, see: Wulff, W. D. In *Comprehensive Organic Synthesis*; Trost, B. M., Fleming, I., Eds.; Pergamon Press: New York, 1990; Vol. 5.

(9) Gleichmann, M. M.; Dötz, K. H.; Hess, B. A. *J. Am. Chem. Soc.* **1996**, *118*, 10551.

**SCHEME 2. Photoreactivity of Chromium Imine–Carbene Complexes with Alkynes**

The value of this reaction as a synthetically useful way to get 2*H*-pyrrole derivatives and as a Dötz-related process prompted us to explore its mechanism. However, due to the difficulties of experimental characterization of the possible reaction intermediates as done in the case of the reaction of imine–carbene complexes with alkenes,<sup>7</sup> we decided to carry out the study of the cyclopentannulation of imine–carbene complexes with alkynes using theoretical tools.

Theoretical calculations of transition-metal complexes are now a well-established tool for the study of organometallic species.<sup>10</sup> Especially important are density functional theory (DFT) methods, due to their expediency, which makes them viable for the study of large-size molecules at a fraction of the time required for post-Hartree–Fock (HF) calculations. An even more important advantage is that in most cases the expectation values derived from approximate DFT are in better agreement with experiment than results obtained from HF calculations. In the particular case of group VI–carbene complexes, DFT methods have shown remarkable agreement with the experimental results.<sup>11</sup> In particular, DFT methods have achieved a number of successes over the past few years in the field of group VI–carbene complex chemistry, as they have been able to reproduce experimental results with considerable accuracy.<sup>12</sup> Encouraged by these results, we tried to apply this methodology to the study of the photochemical cyclopentannulation of imine–carbene complexes with alkynes to make up for the difficulties in the experimental characterization of the intermediates involved.

The general accepted mechanism<sup>4</sup> for the photochemical reactions of Fischer carbene complexes with unsaturated systems involves CO insertion into the Cr=C bond in the first step to form a coordinated ketene followed by reaction with the substrate. This ketene-complex participation determines the formation of benzannulation or cyclobutannulation products. In contrast with this result, we have recently reported the first example of the photochemically induced [3 + 2] cyclopentannulation of imine–group VI carbene complexes with alkynes, which gives 2*H*-pyrrole derivatives (Scheme 2). In these cases, the absence of the CO ligand on the pyrrole structure could indicate an initial CO loss instead of ketene-complex formation after irradiation of carbene complexes. To test this hypothesis, we checked that irradiation of carbene complexes in the presence of Ph<sub>3</sub>P leads to the substitution of one CO by the phosphine ligand.<sup>13</sup>

(10) For a review see: Niu, S.; Hall, M. B. *Chem. Rev.* **2000**, *100*, 353.

(11) For a review, see: Ziegler, T. *Chem. Rev.* **1991**, *91*, 651.

(12) (a) Tafipolsky, M.; Scherer, W.; Ofele, K.; Artus, G.; Pedersen, B.; Herrmann, W. A.; McGrady, G. S. *J. Am. Chem. Soc.* **2002**, *124*, 5865. (b) Torrent, M.; Duran, M.; Solà, M. *J. Chem. Soc., Chem. Commun.* **1998**, 999. (c) Torrent, M.; Duran, M.; Solà, M. *Organometallics* **1998**, *17*, 1492. (d) Wang, C.-C.; Wang, Y.; Liu, H.-J.; Lin, K.-J.; Chou, L.-K.; Chan, K.-S. *J. Phys. Chem. A* **1997**, *101*, 8887. (e) Jacobsen, H.; Ziegler, T. *Organometallics* **1995**, *14*, 224. (f) Jacobsen, H.; Schreckenbach, G.; Ziegler, T. *J. Phys. Chem.* **1994**, *98*, 11406.

At this point, one wonders whether the light effect is only that of opening an empty coordination site by CO dissociation or whether some of the subsequent steps leading to the pyrrole derivative are also involved. Taking into account that thermal reactions have been described for some imine–carbene complexes,<sup>14</sup> we carried out its irradiation in the presence of alkynes. Since our results seem analogous to those previously described, we assume that after CO dissociation the reaction takes place on the ground-state surface; that is, the light effect in this reaction only consists of the activation of the carbene complexes by creating an empty coordination site, which can be filled by the alkyne. This suggests that all the subsequent steps leading to the pyrrole formation should take place on the ground state.

**Computation Methods**

The size of the imine–carbene complex under study necessitated the use of (CO)<sub>5</sub>Cr=CHN=CH<sub>2</sub> and HC≡CH as models for the calculations. All calculations were carried out using the Gaussian 98 program package.<sup>15</sup> Since the DFT method combines the importance of including electron correlation effects and the possibility of dealing with large systems, ground-state molecular geometries were optimized within the nonlocal density approximation (NLDA), including Becke's<sup>16</sup> nonlocal exchange corrections as well as Perdew's<sup>17</sup> inhomogeneous gradient corrections for correlation. For C, O, N, and H, the standard split-valence 6-31G\* basis set<sup>18</sup> was employed. For the chromium atom, we used the Hay–Wadt effective core potential,<sup>19</sup> with the minimal basis set split to [341/2111/41].<sup>20</sup> This basis set has proved its ability to perform calculations on transition-metal complexes with good accuracy.<sup>21</sup> Geometry was fully opti-

(13) Details will be published elsewhere.

(14) (a) Dragisich, V.; Wulff, W. D.; Hoogsteen, K. *Organometallics* **1990**, *9*, 2867. (b) Dragisich, V.; Murray, C. K.; Warner, B. P.; Wulff, W. D.; Yang, D. C. *J. Am. Chem. Soc.* **1990**, *112*, 1251. (c) Aumann, R.; Heinen, H. *J. Organomet. Chem.* **1990**, *389*, C1. (d) Aumann, R.; Heinen, H. *J. Organomet. Chem.* **1990**, *391*, C7.

(15) Gaussian 98, Revision A.7: Frisch, M. J.; Trucks, G. W.; Schlegel, H. B.; Scuseria, G. E.; Robb, M. A.; Cheeseman, J. R.; Zakrzewski, V. G.; Montgomery, J. A., Jr.; Stratmann, R. E.; Burant, J. C.; Dapprich, S.; Millam, J. M.; Daniels, A. D.; Kudin, K. N.; Strain, M. C.; Farkas, O.; Tomasi, J.; Barone, V.; Cossi, M.; Cammi, R.; Mennucci, B.; Pomelli, C.; Adamo, C.; Clifford, S.; Ochterski, J.; Petersson, G. A.; Ayala, P. Y.; Cui, Q.; Morokuma, K.; Malick, D. K.; Rabuck, A. D.; Raghavachari, K.; Foresman, J. B.; Cioslowski, J.; Ortiz, J. V.; Baboul, A. G.; Stefanov, B. B.; Liu, G.; Liashenko, A.; Piskorz, P.; Komaromi, I.; Gomperts, R.; Martin, R. L.; Fox, D. J.; Keith, T.; Al-Laham, M. A.; Peng, C. Y.; Nanayakkara, A.; Gonzalez, C.; Challacombe, M.; Gill, P. M. W.; Johnson, B.; Chen, W.; Wong, M. W.; Andres, J. L.; Gonzalez, M.; Head-Gordon, M.; Replogle, E. S.; Pople, J. A. Gaussian, Inc., Pittsburgh, PA, 1998.

(16) Becke, A. D. *Phys. Rev.* **1988**, *A38*, 3098.

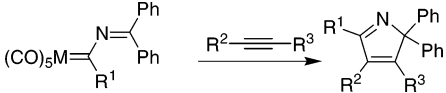
(17) Perdew, J. P. *Phys. Rev.* **1986**, *B33*, 8822; **1986**, *B34*, 7406E.

(18) (a) Hariharan, P. C.; Pople, J. A. *Theor. Chim. Acta* **1973**, *28*, 213. (b) Hehre, W. J.; Ditchfield, R.; Pople, J. A. *J. Chem. Phys.* **1972**, *56*, 2257.

(19) Hay, P. J.; Wadt, W. R. *J. Chem. Phys.* **1985**, *82*, 299.

(20) Frenking, G.; Antes, I.; Böhme, M.; Dapprich, S.; Ehlers, A. W.; Jonas, V.; Neuhaus, A.; Otto, M.; Stegmann, R.; Veldkamp, A.; Vyboishchikov, S. F. In *Reviews in Computational Chemistry*; Lipkowitz, K. B.; Boyd, D. B., Eds.; VCH: New York, 1996; Vol. 8, p 63.

(21) (a) Fernández, E. J.; López-de-Luzuriaga, J. M.; Monge, M.; Rodríguez, M. A.; Crespo, O.; Gimeno, M. C.; Laguna, A.; Jones, P. G. *Chem. Eur. J.* **2000**, *6*, 636. (b) Barluenga, J.; Rodríguez, F.; Vadeкарd, J.; Bendix, M.; Fañanás, F. J.; López-Ortiz, F.; Rodríguez, M. A. *J. Am. Chem. Soc.* **1999**, *121*, 8776. (c) Fernández, E. J.; López-de-Luzuriaga, J. M.; Monge, M.; Rodríguez, M. A.; Crespo, O.; Gimeno, M. C.; Laguna, A.; Jones, P. G. *Inorg. Chem.* **1998**, *37*, 6002.

**TABLE 1.** 2*H*-Pyrrole Derivative Formation through Photoreaction of Imine–Carbene Complexes and Alkynes


entry	M	complex	R <sup>1</sup>	R <sup>2</sup>	R <sup>3</sup>	<i>t</i> (h)	product	yield (%)
1	Cr	<b>1</b>	Me	Ph	Ph	5	<b>5</b>	51
2	Cr	<b>2</b>	Ph	Ph	Ph	5	<b>6</b>	49
3	Mo	<b>3</b>	Me	Ph	Ph	7	<b>5</b>	21
4	Cr	<b>1</b>	Me	Ph	H	5	<b>7</b>	43 <sup>a,b</sup>
5	Cr	<b>1</b>	Me	CO <sub>2</sub> Me	CO <sub>2</sub> Me	11	<b>8</b>	23
6	Cr	<b>1</b>	Me	OEt	H	5	<b>9</b>	73 <sup>a</sup>
7	W	<b>4</b>	Me	OEt	H	5	<b>9</b>	63 <sup>a</sup>

<sup>a</sup> Only one regioisomer was found on the reaction crude. <sup>b</sup> The regiochemistry was wrongly assigned in ref 5.

mized without any symmetry constraint employing Schlegel's analytical gradient procedure,<sup>22</sup> and the optimized structures were characterized as minima or saddle points by analytic frequency calculations, which also allowed the obtaining of ZPE and thermal corrections.<sup>23</sup> Searches for transition states connecting minima were carried out by quadratic synchronous transit approach (QST2).

## Experimental Results

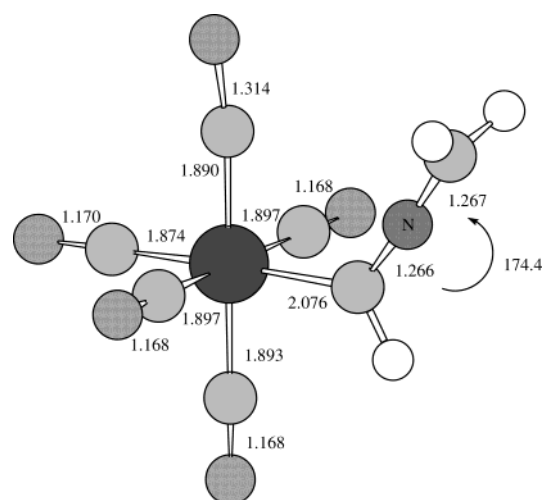
First, we prepared<sup>5</sup> the imine–carbene complexes **1–4** (see Table 1) and carried out the direct irradiation in the presence of alkynes using a series of different substitution patterns. We tested the reaction in a variety of solvent and reagent concentrations. The best results were obtained when we irradiated, with a medium-pressure Hg lamp, 0.25 mmol of imine–carbene complexes in hexane together with 10 equiv of alkyne, through a Pyrex glass. The use of THF, ether, or acetonitrile did not affect the product distribution but increased the polymer formation on the crude. A higher concentration on the starting carbene complex or a lower concentration on the alkyne caused the appearance of metathesis as a side reaction.<sup>5</sup> This can be completely avoided by using the appropriate concentrations. The results are shown in Table 1.

The reaction proceeds in a synthetically useful way, especially in those cases where the alkyne has electron-donating groups. The three group VI metals were tested, and the same qualitative results were found, as all three are capable of producing the cycloaddition with alkynes. However, from a practical point of view, the use of chromium carbenes is recommended, due to the higher yields obtained and the stability of the starting carbene. The final products can be modified by changing the carbenic carbon substituent and the alkyne substituents. This way, the 2*H*-pyrrole obtained can bear different substituents at the 3, 4, and 5 positions. Isomerization to pyrrole is prevented by the two phenyl groups located on the initial carbene's iminic carbon.<sup>24</sup> The regiochemistry of the reaction was determined by X-ray diffraction of one of the 2*H*-pyrrole derivatives formed (**9**, see the

**TABLE 2.** Absolute and Relative Energies of Calculated Structures

compd	total energy (hartrees)	relative energy (kcal/mol)
<b>11</b>	-749.866 147	0.0
<b>TS-12</b>	-749.854 281	+7.4
<b>12</b>	-749.898 810	-20.5
<b>13</b>	-825.146 906	0.0 <sup>a</sup>
<b>14</b>	-825.124 392	+14.1 <sup>a</sup>
<b>13-v</b>	-827.287 927	0.0 <sup>b</sup>
<b>14-v</b>	-827.308 506	+12.9 <sup>b</sup>
<b>TS-15</b>	-749.868 247	-1.3
<b>15</b>	-749.885 259	-12.0
<b>TS-16</b>	-749.860 088	+3.8
<b>16</b>	-749.875 899	-6.1
<b>TS-17</b>	-749.866 925	-0.5
<b>17</b>	-749.903 637	-23.5
<b>TS-18</b>	-749.875 635	-5.9
<b>18</b>	-749.964 735	-61.9

<sup>a</sup> Relative to **13**. <sup>b</sup> Relative to **13-v**.

**FIGURE 1.** Geometrical parameters (bond lengths in Å and angles in deg) of model carbene (CO)<sub>5</sub>Cr=CHN=CH<sub>2</sub> (**10**).

Supporting Information). In **7**, the regiochemistry was assigned on the basis of the analogy of their <sup>1</sup>H and <sup>13</sup>C NMR spectra with that of **9**.

In an effort to work out the reaction mechanism, we looked for reaction intermediates at shorter reaction times. Unfortunately, we were unable to find any species that could help to clarify the mechanism. At this point, we decided to try studying the mechanism of the photocycloaddition by means of theoretical calculations.

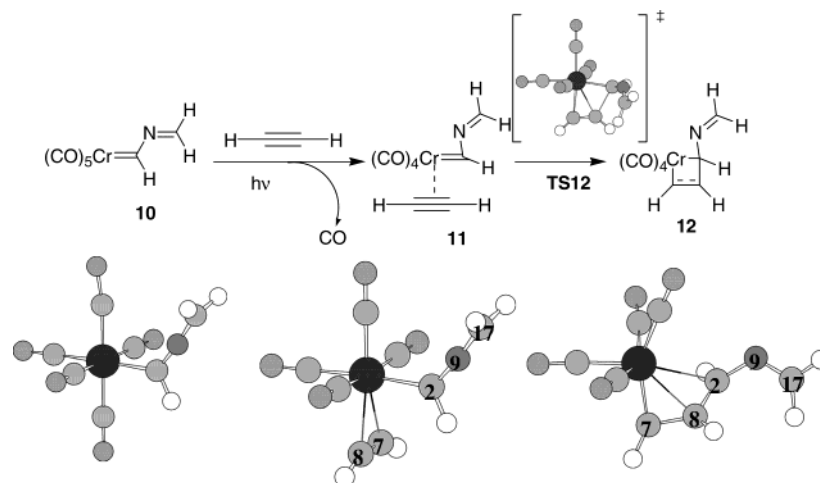
## Theoretical Results

The structures for all the minima and transition states described in the paper are shown in the Supporting Information, with the energies in Table 2. As the first test for the accuracy of the calculations, we optimized the geometry of a model compound of the carbene complexes used. The most relevant geometrical parameters of the optimized structure of (CO)<sub>5</sub>Cr=CHN=CH<sub>2</sub> (**10**) are given in Figure 1. The Cr=C(carbene) distance is 2.076 Å, and the Cr–CO distances are between 1.874 and 1.897 Å, which reflect the weaker π-acceptor character of the carbene ligand as compared to CO. The C(carbene)–N and N–C(imine) bond lengths (1.266 and

(22) Schlegel, H. B. *J. Comput. Chem.* **1982**, *3*, 214.

(23) Hehre, W. J.; Radom, L.; Schleyer, P. V. R.; Pople, J. A. *Ab Initio Molecular Orbital Theory*; J. Wiley: New York, 1986.

(24) Details about the reaction of imine-carbene complexes bearing different substituents on this position will be published elsewhere.

SCHEME 3. Formation of Metallacycle **12**

1.267 Å, respectively) are those of an N=C double bond (1.28 Å), and consistently, the C–N–C bond angle is 174.4°. The calculated structure is in good agreement with the crystal structure of imine–carbene complex **1** (see the Supporting Information). In the molecular structure of complex **1**, distances of 2.113, 1.259, and 1.282 Å are found for the Cr=C(carbene), C(carbene)–N, and N–C(imine) bond lengths, respectively, together with a C–N–C bond angle of 167.5°.

**Alkyne Insertion.** Having checked the accuracy of the method used for the calculations, at least with regard to the structure of the carbene complexes, we aimed to explore the reaction between the carbene complexes and the alkynes. As discussed above, we studied the reaction on the ground state and assume that the role of the light on this process is restricted only to producing the empty coordination position needed for the alkyne.<sup>25</sup> Therefore, the first step on the reaction path should be the substitution of one of the CO ligands by an alkyne, as shown by the experiment of ligand photosubstitution with phosphine.<sup>13</sup> This is in agreement with the two first steps on the proposed mechanism for the Dötz benzannulation, the loss of a CO ligand<sup>26</sup> followed by the alkyne coordination.<sup>27</sup> Taking this into account, we calculated the reaction path from the alkyne-coordinated carbene complex **11** to the final 2*H*-pyrrole formation. The first step on the calculated path is the insertion of the alkyne onto the metal–carbon bond (Scheme 3). This step also appears in the proposed mechanism for the benzannulation and has been found by theoretical calculations to be barrierless<sup>28</sup> or with low energy barriers.<sup>29</sup> As a consequence, the alkyne complex **11** is taken to be a very elusive intermediate that immediately rearranges to give the insertion product **12**. Our calculations show that the transition state **TS-12** that leads from the alkyne-

coordinated complex **11** to the insertion product **12** also has a low energy barrier, in this case 7.4 kcal/mol. The structures for **11**, **TS-12**, and **12** are also shown in Scheme 3. The alkyne moiety is completely symmetrical in the complex **11**, with both Cr–C(alkyne) distances equal to 2.249 Å. The coordination with the metal center clearly deforms the alkyne geometry, producing a C<sub>7</sub>–C<sub>8</sub> distance of 1.254 Å and a H–C<sub>7</sub>–C<sub>8</sub> angle of 156.9°, while the carbene ligand maintains its geometry. From **11**, the main geometrical change needed to arrive at **TS-12** is the rotation of the alkyne ligand. In **11**, the dihedral angle between the planes of the two ligands is almost 90°, with distances between the carbenic carbon C<sub>2</sub> and the two alkyne carbons C<sub>7</sub> or C<sub>8</sub> of 2.923 Å. In **TS-12**, the alkyne ligand is rotated to form an almost planar substructure with the carbenic carbon and the metal center. This rotation is needed to permit the interaction between the two ligands, alkyne and carbenic carbon. The bond distances give an idea about the progression of the alkyne insertion. With regard to the alkyne ligand, one Cr–C distance increases, while the other distance decreases. At the same time, the C<sub>7</sub>–C<sub>8</sub> distance lengthens from 1.254 to 1.290 Å. Clearly, the rotation of the alkyne ligand causes a change in the bond order between it and the chromium atom. The symmetry in compound **12** is broken, and one alkyne carbon, C<sub>7</sub>, interacts strongly with the metal while the other, C<sub>8</sub>, approaches the carbene carbon C<sub>2</sub>. In addition, the carbene moiety is also altered by the increasing interaction with the alkyne. It must also rotate to permit the bond formation, and its linearity decreases as the conjugation is broken due to formation of the C<sub>8</sub>–C<sub>2</sub> bond. The insertion process progresses with the lengthening of the C<sub>2</sub>–Cr and C<sub>7</sub>–C<sub>8</sub> distances and the shortening of the two forming bonds, C<sub>7</sub>–Cr and C<sub>8</sub>–C<sub>2</sub>.

At this point, previous suggestions and studies on this kind of reaction clearly differ from the present work, due to the structure of the insertion product. The postulated intermediate corresponds to a new carbene complex formed by *complete* insertion of the alkyne into the carbenic bond.<sup>29b,30</sup> However, as shown in Scheme 3, the structure for the intermediate which appears after the alkyne coordination is that of a  $\eta^3$  vinylcarbene complex,

(25) Arrieta, A.; Cossío, F. P.; Fernández, I.; Gómez-Gallego, M.; Lecea, B.; Mancheño, M. J.; Sierra, M. A. *J. Am. Chem. Soc.* **2000**, *122*, 11509.

(26) Fischer, H.; Mühlemeier, J.; Märkl, R.; Dötz, K. H. *Chem. Ber.* **1982**, *115*, 1355.

(27) Dötz, K. H.; Siemoneit, S.; Hohmann, F.; Nieger, M. *J. Organomet. Chem.* **1997**, *541*, 285.

(28) Torrent, M.; Duran, M.; Solà, M. *Organometallics* **1998**, *17*, 1492.

(29) (a) Gleichmann, M. M.; Dötz, K. H.; Hess, B. A. *J. Am. Chem. Soc.* **1996**, *118*, 10551. (b) Hofmann, P.; Hämmerle, M. *Angew. Chem., Int. Ed. Engl.* **1989**, *28*, 908.

(30) Dötz, K. H. *Angew. Chem., Int. Ed. Engl.* **1984**, *23*, 587.

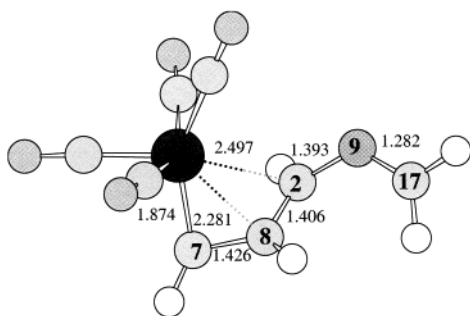


**FIGURE 2.** Geometrical parameters (bond lengths in Å) of imine-carbene complex **12**.

where alkyne insertion has not completed; that is, the alkyne and carbenic carbons ( $C_7$ ,  $C_8$ , and  $C_2$ ) are bonded to the metal center. We propose that it is this, and not the  $\eta^1$  carbene formed through a complete insertion, that is the key intermediate of the *2H*-pyrrole formation. However, this kind of intermediate has not received much attention despite the fact that it has been found both experimentally<sup>31</sup> and theoretically.<sup>32</sup>

The structure of the intermediate **12** shows that three carbon atoms are coordinated to the metal, although the degree of bond order varies greatly (Figure 2). The shorter distance (1.874 Å) corresponds to one of the C atoms from the alkyne ( $C_7$ ). This distance is within the range for a Cr=C bond, which suggests that the insertion of the alkyne into the Cr=C bond is almost completed. However, the other two Cr-C distances (2.281 and 2.497 Å for  $C_8$  and  $C_2$ , respectively) also indicate an interaction between the atoms, thus suggesting that the insertion has not proceeded completely. The angles around  $C_2$  and  $C_8$  have values close to those of  $sp^2$  (125.2° for  $N_9-C_2-C_8$  and 119.7° for the  $C_7-C_8-C_2$ ), although the three C atoms clearly show pyramidalization to some extent. In the same way, the distances between the C atoms ( $C_2-C_8$  1.406 Å and  $C_7-C_8$  1.426 Å) show values between the typical C=C and C-C bond distances. The carbene moiety is twisted with a dihedral angle Cr- $C_7$ - $C_8$ - $C_2$  of 52.8°, as against a twisting of the imine group through a 48.4° dihedral angle on the  $C_8-C_2-N_9-C_{17}$  subsystem, thus making  $\pi$ -conjugation throughout the molecule difficult. Consistently, the bond distances around the  $N_9$  (1.393 and 1.282 Å) clearly correspond to single and double N-C bond distances, respectively.

In a recent paper,<sup>32</sup> Solà et al. found a minimum with a similar structure as an intermediate of the Dötz reaction. However, far from being the global minimum in the reaction's first steps, it is located 11.8 kcal/mol higher in energy than the corresponding  $\eta^1$  complex, with a 16.0 kcal/mol barrier to be passed. The reaction mechanism proposed by Solà consists of the formation of the more stable  $\eta^1$  complex, which later rearranges to the less stable  $\eta^3$  complex, finally progressing to yield the benzannulation product. However it is worth pointing out that this path supposes higher energy than the one the authors proposed as the preferred one. In contrast with Solà's results, structures such as **12** appear to be a

minimum on the potential energy surface for the reaction of imine-carbene complexes with alkynes. The main difference is the location of the N atom, which is directly bonded to the carbenic carbon on structure **12** but via the O atom in Solà's proposal. It may be that the nitrogen's lower electronegativity could permit an increased sharing of its lone pair, in comparison with the oxygen atom. The effect of the N atom substitution causes a decrease in the Cr-C(carbene) distance from 2.630 Å, on the structure calculated by Solà, to 2.497 Å on **12**. Furthermore, the two distances between the three carbons bonded to the chromium atom are slightly shorter for **12** (from 1.428 and 1.415 Å to 1.426 and 1.406 Å for  $C_7-C_8$  and  $C_8-C_2$  in **12**, respectively), suggesting a higher bond order between the four atoms forming the *metallacyclobutene*. These changes may account for the increased stability of our complex, which therefore becomes a real minimum on the reaction course. As an additional point, some years ago the Barluenga<sup>31</sup> group was able to isolate and fully characterize by X-ray diffraction a carbene complex with similar structure, also with a N atom next to one of the C atoms directly bonded to the metal center. This result clearly shows that the N atom causes a stabilization on this kind of intermediates, which become stable enough to be trapped. On the other hand, the absence of the N atom leads to a higher energy intermediate, as Solà's calculations show, causing the reaction path to diverge at this point from the one proposed by the Dötz benzannulation.

Next, we were interested in the influence of the metal on the reaction. It is not unusual to find a quite different behavior between the complexes of these two metals in the literature.<sup>1</sup> Cases have been reported where the product distribution differs greatly according to the use of W or Cr as the metal center.<sup>33</sup> However, the reaction between imine-carbene complexes and alkynes shows that the synthesis and reactivity of imine-carbene complexes with tungsten or chromium are broadly similar, so allowing a wider applicability range on a synthetic way. The similarity could mean that the metal does not exert a strong influence on the reaction path, that is, that the key intermediates have similar structures. To test this hypothesis we computed the analogue complex **12-W**, replacing the chromium atom with a tungsten atom. The resulting structure is very similar, apart from the slightly longer W-C distances due to the metal's differing characteristics (see the Supporting Information).

On the other hand, as discussed above, the reaction is completely regioselective (see Table 1, entries 4, 6, and 7). The alkyne moiety is completely symmetric in complex **11**, while in the alkyne insertion product **12**, this symmetry is broken. This step could therefore be responsible for the reaction's regiochemistry. Once the alkyne complex has been formed, the presence of different groups on the alkyne will lead to different insertion products, causing the generation of two different products with opposite regiochemistries. The experimental results suggest that one of these products should be favored in some way. To test this hypothesis, we calculated the two insertion products produced from the model carbene

(31) Barluenga, J.; Aznar, F.; Martín, A.; García-Granda, S.; Pérez-Carreño, E. *J. Am. Chem. Soc.* **1994**, *116*, 11191.

(32) Torrent, M.; Duran, M.; Solà, M. *J. Am. Chem. Soc.* **1999**, *121*, 1309.

(33) For some examples see: (a) Bertolini, T. M.; Nguyen, Q. H.; Harvey, D. F. *J. Org. Chem.* **2002**, *67*, 8675. (b) Barluenga, J.; Aznar, F.; Martín, A.; Barluenga, S. *Tetrahedron* **1997**, *53*, 9323. (c) Harvey, D. F.; Lund, K. P. *J. Am. Chem. Soc.* **1991**, *113*, 5066.

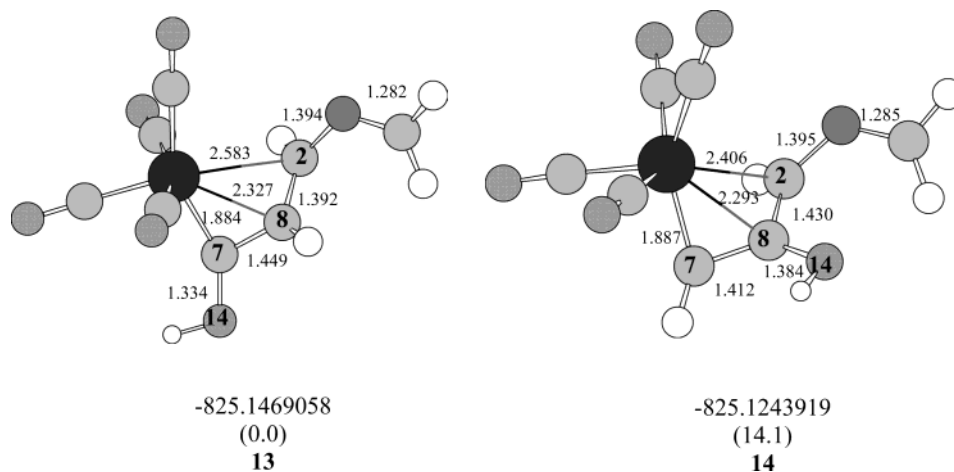


**FIGURE 3.** Geometrical parameters (bond lengths in Å) and absolute (hartrees) and relative (in parentheses, kcal/mol) energies of the two regioisomeric products of the alkyne HC≡COH insertion.

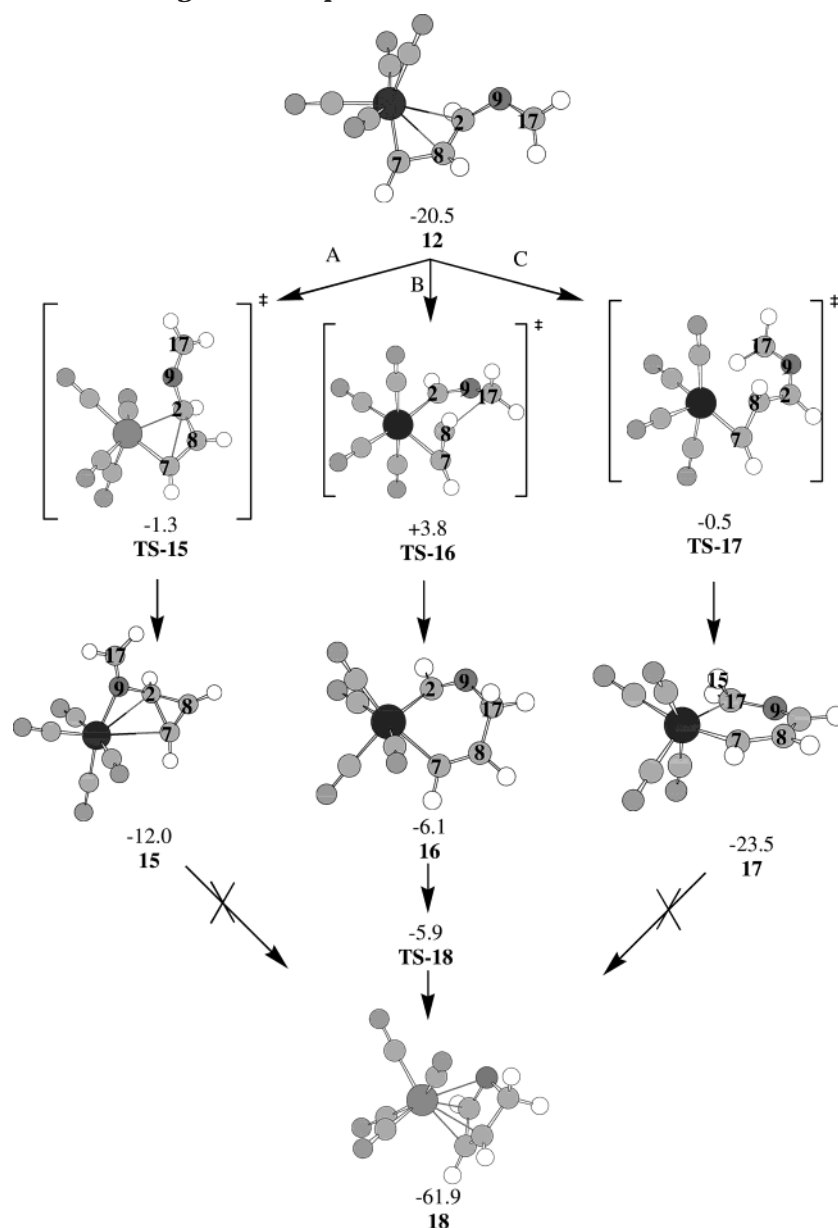
complex and H-C≡C-OH. We then used this to reproduce the reaction between carbene complex **1** and ethynyl ethyl ether (see Table 1, entry 6). We were able to find the two structures (**13** and **14**) analogous to the compound **12**, shown in Figure 3.

The two intermediates have similar structures; however, they clearly differ in the bond distances of the metallacyclobutene. The main difference seems to be the degree of progression of the alkyne insertion, with structure **13** showing almost complete insertion, with a Cr-C<sub>2</sub> distance of 2.583 Å. Also, the two bonds around C<sub>8</sub> have rather different distances (1.449 and 1.392 Å) indicating a poor delocalization along the cycle. On the other hand, **14** shows bond lengths more similar to the compound **12**, with shorter Cr-C<sub>2</sub> distance (2.406 Å) and similar bond distances around C<sub>8</sub> (1.412 and 1.430 Å). The effect of introducing an oxygen atom can be clearly seen from the C-O distances. In **13**, the C<sub>7</sub>-O<sub>14</sub> is 1.334 Å, while the corresponding distance (C<sub>8</sub>-O<sub>14</sub>) in **14** is 1.384 Å. This variation illustrates the true difference between these two systems; when the oxygen atom is located next to the carbon atom close to the metal, this contributes to a net stabilization of the compound. This is a well-known feature of the Fischer carbene complexes, where the placement of an atom with a lone pair (O, N, S, etc.) onto the carbenic carbon allows the presence of a resonance form which greatly increases the stability of the compound.<sup>1</sup> In this case, the presence of the O atom causes a major difference in the stability of the two insertion products. The difference of 14.1 kcal/mol should be enough to lead to the formation of *only one* insertion regioisomer. Thus, this result can account for the product distribution found experimentally, where just one regioisomer was found in the case of the reaction with ethynyl ethyl ether. Equally, substitution of the hydroxyl by a vinyl group (HC≡CCH=CH<sub>2</sub> as alkyne model) affords the same results. We calculated the equivalent products **13-v** and **14-v** (see the Supporting Information), where we tried to mimic the influence of the phenyl groups using vinyl substituents. The same regiochemistry is also expected for conjugated alkynes such as phenyl acetylene used in entry 4, Table 1. Compound **13-v** is around 13

kcal/mol more stable than **14-v** (see Table 2), and the bond distances show values similar to those for **13** and **14**.

Once the metallacyclobutene intermediate has been reached, and given that the reaction yields a 2*H*-pyrrole derivative as the only detectable product, a ring enlargement should occur between this point and the final product formation. Also, a reductive elimination should occur to generate the organic compound without the metal part. Three different possibilities were considered, depending on the chronological order of these steps: ring enlargement, reductive elimination, and the regiochemistry of the ring enlargement. The three possible paths are shown in Scheme 4. In routes B and C, the ring enlargement takes place immediately after the metallacyclobutene formation, generating a six-membered metallacycle, which, in a subsequent step, undergoes the reductive elimination; there is a difference between the two routes as regards the regiochemistry of the ring enlargement. In route A, the ring enlargement takes place after the reductive elimination. Taking the metallacyclobutene **12** as a starting point, we calculated these three paths, including the transition structures involved. As can be seen in Scheme 4, although the three paths have to go through transition structures of a comparable height (19.2 kcal/mol for route A, 24.3 kcal/mol for route B, and 20.0 kcal/mol for route C), the main difference between them is the relative energies of the final products. While the cyclopropene **15** generated through route A is 8.5 kcal/mol higher in energy than the previous intermediate **12**, the final 2*H*-pyrrole **18** formed through route B is 41.4 kcal/mol more stable. This difference should be enough to lead to the formation of the pyrrole derivatives through route B, producing a ring enlargement of compound **12** followed by a reductive elimination. Finally, **17** is 37.4 kcal/mol less stable than **18**.

**The Cyclopropene Route.** The transition state for the route A, **TS-15**, leading to the cyclopropene **15** presents a structure related to that of the intermediate **12**, but is placed 19.2 kcal/mol above. The bond distances show the movements needed to complete the reductive elimination. The C<sub>7</sub>-C<sub>8</sub> distance is clearly shorter (1.346 Å) with a characteristic C=C value. This is caused by

SCHEME 4. Three Routes Starting from Compound **12**<sup>a</sup>

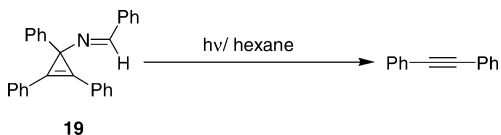
<sup>a</sup> Relative energies in kcal/mol.

the absence of conjugation resulting from the breakage of the Cr–C<sub>2</sub> bond at the same time as the C<sub>7</sub>–C<sub>2</sub> bond is forming. The shorter Cr–C<sub>2</sub> distance is simply a geometrical requirement which permits the formation of the cyclopropene. The metallacycle breakage can also be seen in the return to planarity of the three C atoms forming the cycle and the metal, again a requirement for cyclopropene formation.

The coordinative needs of the chromium atom in **15** are fulfilled by coordination of the nitrogen atom N<sub>9</sub>. The last coordination site is partially taken up by the cyclopropene unit. However, the ring-closing geometry means that the double bond C<sub>7</sub>–C<sub>8</sub> does not have the right orientation to allow the bonding with the metal. In this situation, it is the newly formed C<sub>7</sub>–C<sub>2</sub> bond which fills this site. This can be clearly seen by comparing the two C–C single bond distances of the cyclopropene moiety (C<sub>2</sub>–C<sub>8</sub> 1.492 Å and C<sub>2</sub>–C<sub>7</sub> 1.547 Å). The second one is

too large for this kind of compound and is a consequence of the coordination to the metal. Intermediate **15** could evolve via two different routes: first, a direct ring enlargement to give **18**, or second, by analogy with the reaction with alkenes (Scheme 1),<sup>7</sup> so involving the loss of the metal part followed by ring enlargement to afford the 2*H*-pyrrole.<sup>34</sup> The first possibility was discounted since we were unable to find any transition structure connecting **15** and **18**. As an indirect proof for the second alternative, and taking into account that *no product with the cyclopropene skeleton could be isolated or detected* in the reaction crude, we synthesized the iminecyclopropene

(34) The photorearrangement of vinylcyclopropene and related compounds to yield five-membered rings is known. See, for example: (a) Zimmerman, H. E.; Wright, C. H. *J. Am. Chem. Soc.* **1992**, *114*, 6603. (b) Zimmerman, H. E.; Fleming, S. A. *J. Org. Chem.* **1985**, *50*, 2539. (c) Padwa, A.; Blacklock, T. J.; Getman, D.; Hatanaka, N. *J. Am. Chem. Soc.* **1977**, *99*, 2344.

**SCHEME 5. Test for the Cyclopropene–Pyrrole Rearrangement**

**19** and we irradiated it under the same reaction conditions (Scheme 5). After some time of irradiation we obtained a complex crude, with tolane as the main product, together with some other unidentified compounds, none of them with pyrrole structure. This result allows us to reject the hypothesis of formation of *2H*-pyrrole derivatives through the mechanism sketched on route A, insofar as (a) **15** is clearly less favorable than **17** or **18**; (b) we were unable to find any TS which could explain the pyrrole formation from **15**; (c) we were unable to isolate or detect any compound with a cyclopropene structure on the reaction crude; (d) the synthesized imine–cyclopropene did not rearrange under the reaction conditions. We see here a clear distinction between the reaction of imine–carbene complexes with alkenes and with alkynes. In the former, the five-membered cycle is generated through two consecutive reactions and the intermediate cyclopropane can be isolated in some cases. In the latter, the pyrrole derivatives are formed directly, and no intermediate can be trapped.

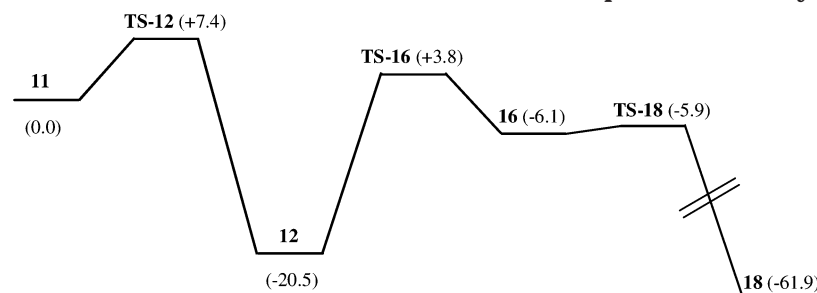
**The Metalladiene Routes.** Routes B and C start from compound **12** and give two different metallacycles through two different ring enlargements (see Scheme 4). The difference between these two possible pathways is the direction of the ring enlargement. We computed both routes from compound **12** to give the six-membered metallacycle in two forms, **16** and **17**. Scheme 4 shows the two different cycles, together with the transition structures leading to them. As can be seen, the two possibilities clearly differ in the relative energies of both minima and transition structures. The two isomeric metallazaahexadienes differ as regards connectivity. In compound **16**, the ring enlargement takes place after the approach of the imine moiety to the cycle from the direction *opposite to the metal center*, with formation of a C<sub>17</sub>–C<sub>8</sub> bond. The corresponding transition state **TS-16** shows a structure intermediate between the two minima **12** and **16**. The bond distances around the N<sub>9</sub> atom reflect these alterations: while the iminic bond lengthens from a C<sub>17</sub>–N<sub>9</sub> value of 1.282 Å in **12** to a C<sub>17</sub>–N<sub>9</sub> distance of 1.306 Å in **TS-16** due to the bond formation between the iminic carbon (C<sub>17</sub>) and C<sub>8</sub> in the cycle, the C<sub>2</sub>–N<sub>9</sub> distance shortens from 1.393 to 1.266 Å, showing the formation of a C=N double bond. At the same time, C<sub>2</sub> approaches the metal center, forming a σ-bond (Cr–C<sub>2</sub> 2.497 Å in **12**, 2.164 Å in **TS-16**, and 2.091 Å in **16**). However, formation of compound **17** requires a more complex conformational change. The imine moiety has to rotate in order to face the metal center. This causes a minor modification in this part of the molecule in the TS (distances around N<sub>9</sub> of 1.282 Å in **12** vs 1.285 Å in **TS-17** and 1.393 Å in **12** vs 1.318 Å in **TS-17**), while the more important change consists of the removal of one of the C atoms in the cycle (C<sub>2</sub>) from the vicinity of the metal center, needed to create a coordinative place for the introduction of the approaching iminic carbon (C<sub>17</sub>) close to the metal.

Compound **16** has two similar Cr–C bond distances (Cr–C<sub>7</sub>, 2.108 Å, and Cr–C<sub>2</sub>, 2.091 Å). This indicates a similar bond order between the metal center and the two carbon atoms. The situation is different in the case of compound **17**, where one of the Cr–C distances is clearly longer than the other (Cr–C<sub>7</sub>, 1.983 Å, vs Cr–C<sub>17</sub>, 2.277 Å). These values suggest different natures for the two complexes. While compound **16** has two single Cr–C bonds, compound **17** presents a double Cr=C<sub>7</sub> bond and a σ interaction with C<sub>17</sub>, which is slight but nonetheless clear enough to be noted via the pyramidalization of the C. At this point, the fate of these two compounds can be postulated on the basis of the bond order found. The compound **16** could yield the corresponding *2H*-pyrrole by reductive elimination of the metal center. The two σ Cr–C bonds would have to be involved in forming the new C<sub>2</sub>–C<sub>7</sub> bond, which yields the final product. This means that compound **16** would be connected with the final product **18** by a transition state 0.2 kcal/mol higher in energy. On the other hand, compound **17** could not give this reductive elimination due to its different bond distribution; thus the pyrrole formation path is blocked. This can be understood by taking a closer look at the structure. The reductive elimination needed to yield the pyrrole derivative is prevented by the slight interaction of the metal center with C<sub>17</sub>. Indeed, the bond order between these two atoms is quite small due to the *agostic interaction* between one hydrogen atom on C<sub>17</sub> and the metal (the Cr–H<sub>15</sub> distance is 1.891 Å, which is a normal value for this kind of interactions).<sup>35</sup> This causes the C<sub>17</sub>–H<sub>15</sub> bond to lengthen considerably: 1.153 Å for the C<sub>17</sub>–H distance with the hydrogen involved in the agostic interaction vs 1.096 Å for the other C<sub>17</sub>–H distance in the same carbon atom. By the way of confirmation, we were unable to find any transition state connecting **17** with the final product **18**. In summary, route C gives metallacycle **17**, whose further development is blocked. Route B leads to metallacycle **16**, which can evolve to the most stable product **18**. Thus, once **16** is formed, **18** is easily produced by reductive elimination of the metal atom, through a transition state 14.6 kcal/mol higher in energy than **12**, that is, only 0.2 kcal/mol above **16**. This means that after the rearrangement from **12** to **16** takes place, the *2H*-pyrrole formation should be immediate. **18** is the most stable species on the reaction path, and its formation should be the driving force for the reaction completion. Looking at the energies of the different transition structures, **TS-12** is the highest one. Once the first and highest transition state (**TS-12**) is passed, the product distribution should be consistently under thermodynamic control. This causes the reaction to be controlled by the relative energies of the final products, that is, the reaction is directed toward the formation of the more stable species, the *2H*-pyrrole derivative with the regiochemistry detected.

The energy profile for this reaction is shown in Scheme 6. As discussed before, only one regioisomer was found on the reaction crude; the reaction path as calculated explains this and the other experimental findings. Several possibilities open up after the alkyne insertion; according to our calculations, the reaction then proceeds through the metallacycle route, with formation of **16**,

(35) Hall, C.; Perutz, R. N. *Chem. Rev.* **1996**, *96*, 3125.



SCHEME 6. Energy Profile for the Reaction of Imine–Carbene Complexes with Alkynes<sup>a</sup>

<sup>a</sup> Relative energies in kcal/mol.

from which the most stable product **18** should be immediately obtained.

### Conclusions

Experimental studies and high level theoretical calculations were done in order to explore the reactivity between imine–carbene chromium complexes and alkynes. Despite the existence of different reaction paths, the relative energies of the intermediates and products involved can account for the product distribution and the regiochemistry experimentally obtained. This reaction has been shown to be an easy and versatile doorway to 2*H*-pyrrole derivatives, as long as the regiochemistry of the final products can be controlled. A different mechanism from that previously proposed for the reaction with alkenes is suggested. Despite the apparent similarities between the reaction of imine–group VI carbene complexes in the presence of alkynes and the Dötz reaction, which include some of the intermediates in common, the calculations show that the reaction mechanisms differ immediately after the alkyne insertion. Once the light opens up a coordination site by CO dissociation, the reaction proceeds through the alkyne insertion, followed by ring enlargement and reductive elimination. Once again, Fischer carbene complexes show their complexity. Related starting materials (alkenes and alkynes) give related products (pyrrolines and 2*H*-pyrroles) through quite different mechanisms.

### Experimental Section

**General Procedure for Irradiation.** The carbene complex (0.25 mmol) was dissolved in 50 mL of deoxygenated hexane. Ten equivalents of alkyne was added, and the mixture was irradiated at room temperature under an Ar atmosphere, through a Pyrex glass with a 125 W medium-pressure mercury lamp, until the carbene was consumed (TLC, hexane/CH<sub>2</sub>Cl<sub>2</sub> 1:1). The solvent was removed with a rotary evaporator, and the crude product was filtered through Celite to remove chromium residues. The product was purified by column chromatography (silica gel, hexane/Et<sub>2</sub>O).

**2-Methyl-3,4,5,5-tetraphenyl-2*H*-pyrrole (5):** yellow solid; yield 49 mg, 51%; <sup>1</sup>H NMR δ 2.30 (s, 3H, CH<sub>3</sub>), 6.8–7.5 (m, 20 H, arom); <sup>13</sup>C NMR δ 18.4 (CH<sub>3</sub>), 90.1 (CPh<sub>2</sub>), 127.3, 127.6, 127.7, 127.8, 128.1, 128.3, 128.5, 128.6, 128.7, 129.3, 129.5, 130.1, 130.8, 134.0, 134.8, 139.5, 139.7, 164.8, 171.9 (C=N); GC–MS 385 (M, 8), 384 (100), 344 (7), 305 (10), 265 (19), 153 (21); ES (+) 386 (M + 1). Anal. Calcd for C<sub>29</sub>H<sub>23</sub>N: C, 90.35; H, 6.01; N, 3.63. Found: C, 90.55; H, 6.10; N, 3.35.

**2,3,4,5,5-Pentaphenyl-2*H*-pyrrole (6):** yellow solid; yield 55 mg, 49%; <sup>1</sup>H NMR δ 6.95–7.88 (m, 25H, arom); <sup>13</sup>C NMR δ 92.2 (CPh<sub>2</sub>), 119.1, 123.5, 125.5, 126.4, 126.5, 127.5, 127.7,

127.8, 128.0, 128.2, 128.3, 128.6, 128.7, 131.2, 132.4, 135.5, 136.7, 138.6, 140.8, 141.2, 147.4, 148.2, 170.1 (C=N); GC–MS 447 (M, 15), 370 (8), 292 (27), 252 (23), 165 (100), 139 (16), 103 (15), 77 (79), 51 (63); ES (+) 448 (M + 1); IR ν 3053 (m), 1712 (s), 1626 (m), 1596 (m), 1577 (m), 1492 (m) cm<sup>-1</sup>. Anal. Calcd for C<sub>34</sub>H<sub>25</sub>N: C, 91.24; H, 5.63; N, 3.13. Found: C, 91.20; H, 5.61; N, 3.19.

**2-Methyl-3,5,5-triphenyl-2*H*-pyrrole (7):** yellow solid; yield 33 mg, 43%; <sup>1</sup>H NMR δ 2.38 (s, 3H, CH<sub>3</sub>), 6.77 (s, 1H, CH), 7.22–7.36 (m, 15H, arom); <sup>13</sup>C NMR δ 18.9, 90.4, 126.2, 126.3, 126.9, 127.2, 127.5, 127.8, 127.9, 128.1, 128.3, 128.4, 128.6, 128.7, 133.5, 139.3, 170.7 (C=N); GC–MS 309 (M, 28), 265 (5), 230 (8), 191 (15), 165 (100), 139 (12), 102 (72), 77 (92), 51 (95); ES (+) 310 (M + 1); IR ν 3684 (w), 3058 (m), 1684 (w), 1619 (m), 1599 (m), 1492 (m). Anal. Calcd for C<sub>23</sub>H<sub>19</sub>N: C, 89.28; H, 6.19; N, 4.53. Found: C, 89.34; H, 6.15; N, 4.51.

**2-Methyl-3,4-di(methoxycarbonyl)-5,5-diphenyl-2*H*-pyrrole (8):** yellow oil; yield 24 mg, 23%; <sup>1</sup>H NMR δ 2.47 (s, 3H, N=CCH<sub>3</sub>), 3.69 (s, 3H, CO<sub>2</sub>CH<sub>3</sub>), 3.88 (s, 3H, CO<sub>2</sub>CH<sub>3</sub>), 7.1–7.4 (m, 10H, arom); <sup>13</sup>C NMR δ 18.3 (N=CCH<sub>3</sub>), 52.4 (CO<sub>2</sub>CH<sub>3</sub>), 52.6 (CO<sub>2</sub>CH<sub>3</sub>), 92.3 (CPh<sub>2</sub>), 127.9, 128.0, 128.1, 128.1, 128.2, 128.3, 128.5, 134.3, 135.6, 138.2, 163.5 (C=O), 163.7 (C=O), 167.9 (C=N); GC–MS 349 (M, 43), 258 (35), 230 (29), 189 (28), 165 (10), 127 (56), 102 (15), 77 (39), 59 (100); ES (+) 350 (M + 1); IR ν 3680 (w), 1737 (s), 1728 (s), 1639 (m) cm<sup>-1</sup>.

**2-Methyl-3-ethoxy-5,5-diphenyl-2*H*-pyrrole (9):** yellow solid; yield 13 mg, 73%; <sup>1</sup>H NMR δ 1.38 (t, *J* = 7 Hz, 3H, CH<sub>2</sub>CH<sub>3</sub>), 2.26 (s, 3H, CH<sub>3</sub>C=N), 3.94 (c, *J* = 7 Hz, 2H, CH<sub>2</sub>CH<sub>3</sub>), 6.40 (s, 1H, CH), 7.1–7.5 (m, 10H, arom); <sup>13</sup>C NMR δ 14.4 (CH<sub>2</sub>CH<sub>3</sub>), 15.6 (CH<sub>3</sub>C=N), 66.2 (CH<sub>2</sub>CH<sub>3</sub>), 83.2 (CPh<sub>2</sub>), 119.8 (C=CO), 126.8, 127.4, 128.0, 142.9, 154.6 (C=CO), 169.1 (C=N); GC–MS 277 (M, 48), 248 (23), 207 (18), 179 (100), 152 (8), 77 (15); ES (+) 278 (M + 1). Anal. Calcd for C<sub>19</sub>H<sub>19</sub>NO: C, 82.28; H, 6.90; N, 5.05. Found: C, 82.38; H, 6.84; N, 5.00.

**Preparation of Cyclopropene 19.** Triphenylcyclopropenium tetrafluoroborate<sup>34b</sup> (1 mmol) was dissolved in 50 mL of dry MeCN. One equivalent of the PhCHO was added. After bubbling NH<sub>3</sub>, the mixture was stirred at room temperature for 1 h. The solvent was removed with a rotary evaporator, and the product was purified by flash column chromatography (silica gel, hexane/Et<sub>2</sub>O). The irradiation procedure was analogous to that previously described for *N*-cyclopropylimines.<sup>7b</sup>

**3-(Phenylmethyleneamino)-1,2,3-diphenylcyclopropene (19):** yellow oil; yield 13 mg, 53%; <sup>1</sup>H NMR δ 7.1–7.5 (m, 12H, arom.), 7.6–7.7 (m, 6H, arom.), 7.8–7.9 (m, 2H, arom.), 8.39 (s, 1H); <sup>13</sup>C NMR δ 116.6, 126.8, 127.4, 128.0, 129.4, 130.0, 130.5, 130.9, 131.8, 132.5, 132.7, 135.7, 142.9, 154.6, 156.1 (C=N); ES (+) 360 (M + 1).

**Crystallographic Data for Pentacarbonyl[methyl-(diphenylmethyleneamino)methylene]chromium (1).** An orange prismatic crystal of **1** (C<sub>20</sub>H<sub>13</sub>CrNO<sub>5</sub>, MW = 399.32) was transferred to the goniostat. The data were collected at room temperature with an Enraf Nonius apparatus with κ geometry and an electronic CCD detector. It was determined to have monoclinic symmetry with a *P2* space group. Unit cell param-

eters are  $a = 12.268 \text{ \AA}$ ,  $b = 7.823 \text{ \AA}$ ,  $c = 19.884 \text{ \AA}$ , and  $\beta = 91.20^\circ$ , and  $D_{\text{calcd}} = 1.309 \text{ g/cm}^3$  for  $Z = 4$ . A total of 4255 unique data were collected for  $1.93^\circ \geq 2\theta \geq 27.44^\circ$ . The structure was solved by direct methods using SHELX97 with a GOF = 1.473. Final residuals are  $R(F) = 0.055$  and  $R_w(F) = 0.1545$ .

**Crystallographic Data for 2-Methyl-3-ethoxy-5, 5-diphenyl-2H-pyrrole (9).** A colorless prismatic crystal of **9** ( $\text{C}_{19}\text{H}_{19}\text{NO}$ , MW = 277.37) was transferred to the goniostat. The data were collected at room temperature with an Enraf Nonius apparatus with  $\kappa$  geometry and an electronic CCD detector. It was determined to have triclinic symmetry with a  $P-1$  space group. Unit cell parameters are  $a = 8.856 \text{ \AA}$ ,  $b = 8.856 \text{ \AA}$ ,  $c = 22.924 \text{ \AA}$ ,  $\alpha = 89.43^\circ$ ,  $\beta = 89.42^\circ$ , and  $\gamma = 62.97^\circ$ , and  $D_{\text{calcd}} = 1.15 \text{ g/cm}^3$  for  $Z = 4$ . A total of 4521 unique data were collected for  $0.99^\circ \geq 2\theta \geq 21.04^\circ$ . The structure was

solved by direct methods using SHELX97 with a GOF = 1.344. Final residuals are  $R(F) = 0.082$  and  $R_w(F) = 0.2133$ .

**Acknowledgment.** This work was supported by Spanish MCyT/FEDER (BQU2001-1625) and Universidad de La Rioja (API-01/B07). D.S. thanks the Spanish Comunidad Autónoma de La Rioja for a fellowship.

**Supporting Information Available:** Cartesian coordinates of all minima and transition structures **10–18**, X-ray data and ORTEP views of compounds **1** and **9**, and general experimental comments. This material is available free of charge via the Internet at <http://pubs.acs.org>.

JO0343073